ELSEVIER

Carbohydrate Polymers 44 (2001) 261–268

Carbohydrate Polymers

www.elsevier.com/locate/carbpol

Hydrodynamic characterisation of the exopolysaccharide from the halophilic cyanobacterium *Aphanothece halophytica* GR02: a comparison with xanthan

G.A. Morris[a,*], P. Li[a,b], M. Puaud[a], Z. Liu[b], J.R. Mitchell[a], S.E. Harding[a]

[a]*School of Biosciences, University of Nottingham, Sutton Bonington, LE12 5RD, UK*

[b]*State Key Laboratory of Pharmaceutical Biotechnology, Department of Biology, Nanjing University, Nanjing, 210093, People's Republic of China*

Accepted 11 April 2000

Abstract

A bacterial exopolysaccharide from *Aphanothece halophytica* GR02 (AH-EPS) solubilised in buffered 1 M guanidine hydrochloride, GuHCl was studied using capillary viscometry, double gap viscometry, sedimentation velocity and sedimentation equilibrium using analytical ultracentrifugation. Results from capillary viscometry indicate that the exopolysaccharide is xanthan-like in its shear thinning properties. This was confirmed by double gap viscometry. Sedimentation velocity (distribution of apparent sedimentation coefficients) confirmed that the AH-EPS solution was reasonably homogeneous and a hyper-sharp boundary indicated that AH-EPS is a rigid/extra-rigid rod type polysaccharide. Sedimentation equilibrium confirmed the high molecular weight indicated by viscosity measurements. In order to ascertain whether the solution physical properties of AH-EPS are xanthan-like under the conditions studied, all the above experiments were repeated on a similarly treated xanthan solution in the same solvent. Results indicate that AH-EPS is indeed xanthan-like in its physical properties at least in the system studied. Xanthan properties in GuHCl do not appear too different from those studied in more traditional solvents.

Keywords: Bacterial exopolysaccharide; *Aphanothece halophytica*; Xanthan-like; Hydrodynamic characterisation; Guanidine hydrochloride; Cross-equation

1. Introduction

It has been known for a long time that Cyanobacteria, the most widely distributed photosynthetic prokaryotes in nature, produce large amounts of exopolysaccharides (see e.g. Drews & Weckesser, 1982). These exopolysaccharides have potential biotechnological importance as conditioners of soils for the improvement of their water-holding capacity, emulsifiers, viscosifiers, medicines and bioflocculants (Bar & Visnovsky 1997; Bar-or & Shilo, 1987; Choi, Yoo, Oh & park, 1998; De Philippis & Vincenzini, 1998; Falchini, Sparvoli & Tomaselli, 1996; Mazor, Kidron, Vonshak & Abeliovich, 1996).

Although the monosaccharidic compositions of exopolysaccharides present in a number of species of cyanobacteria have been determined (De Philippis & Vincenzini, 1998; Nicolaus et al., 1999), further studies are necessary to understand and assess the biotechnological potential of cyanobacterial exopolysaccharide. Indeed, only a few papers have dealt with the physico-chemical and structural studies. Their data has suggested that the solution conformation of exopolysaccharide from *Cyanospira capsulata* (CC-EPS) is a random coil (Cesaro, Liut, Bertocchi, Navarini & Urbani, 1990; Navarini, Cesaro & Ross-Murphy, 1992). Aqueous solutions of CC-EPS show good rheological properties, just about equivalent to those of xanthan (Cesaro et al., 1990; Navarini, Bertocchi, Cesaro, Lapasin & Crescenzi, 1990). CC-EPS is a regular branched acidic polysaccharide with a decasaccharide (Marra, Palmeri, Ballio, Segre & Slodki, 1990) or octasaccharide repeating unit (Garozzo, Impallomeni, Spina & Sturiale, 1998).

Aphanothece halophytica is one of the few halophilic cyanobacteria (Brock, 1976). *Aphanothece halophytica* GR02, is usually a benthic cyanobacterium in the Guangrao saltworks, which often forms surface water blooms. After the bloom formation, the brine of the saltworks gradually becomes viscous due to of the release of large amounts of exopolysaccharide from *A. halophytica* GR02 (AH-EPS) (Liu & Lin, 1993). AH-EPS consists mainly of glucose, fucose, mannose, arabinose and glucuronic acid. A possible backbone of AH-EPS contains glucose, arabinose, fucose, mannose and glucuronic acid with branch points at

* Corresponding author. Tel.: +44-115-9516198; fax: +44-115-9516142.

E-mail address: scxgam@nottingham.ac.uk (G.A. Morris).

0144-8617/01/$ - see front matter
PII: S0144-8617(00)00217-4

mannose, and the remaining glucose and glucuronic acids are at terminal positions. No peptide or sulphate residues were detected (Li, Liu, Xu & Zhu, 2000).

Xanthan, an exopolysaccharide from *Xanthomonas campestris*, has been extensively studied. Xanthan has gained widespread use as a viscosifier in a number of different commercial applications (Dhami, Harding, Jones, Hughes, Mitchell & To, 1995), including many food applications, where it was approved in the EC in 1980 under the name E415.

In this paper we report a comparative hydrodynamic study on the dilute solution and rheological properties of the exopolysaccharide produced by the halophilic cyanobacterium *A. halophytica* GR02 and xanthan in guanidine hydrochloride, GuHCl solvent. To our knowledge, this is the first report on the hydrodynamic characterisation of the exopolysaccharide from the cyanobacterium.

2. Materials and methods

2.1. Sample preparation

A. halophytica GR02 was isolated from the Guangrao saltwork in the Shandong province of People's Republic of China. After 20 days growth, the cells were removed by centrifugation, and the supernatant filtered through a 0.45 μm porous membrane, and then concentrated under reduced pressure at 40°C. Sodium azide was added to prevent bacterial growth, this concentrated medium was then dialysed against tap water (60 h) and distilled water (18 hours) and then concentrated again. The exopolysaccharides were then precipitated by the addition of four volumes of 95% ethanol at 4°C overnight (Li et al., 2000).

The resulting dried exopolysaccharide sample then proved difficult to dissolve. Many typical aqueous solvents used in hydrodynamic characterisations were tested for their effectiveness as a solvating agent, including "Paley" buffers of differing pHs (Green, 1933), DMSO and ethanol. These solvents, however, proved ineffective. It was found that only after several days stirring at room temperature in 1 M guanidine hydrochloride, GuHCl was a reasonably homogeneous solution formed. Therefore all subsequent analyses were carried out in this medium. 1 M GuHCl also suppresses any microbiological growth. For comparison xanthan samples were also dissolved in 1 M GuHCl.

2.2. Capillary viscometry

Solutions and reference solvents were analysed using a 2 ml automatic Schott-Geräte Oswald viscometer, under precise temperature control (24.96 ± 0.01°C). The relative, η_{rel} specific, η_{sp} and reduced, η_{red} viscosities were calculated from

$$\eta_{rel} = (t/t_0)\cdot(\rho/\rho_0) \quad (1)$$

where t is the flow time for the polysaccharide sample, t_0 the flow time for the solvent (81.95 ± 0.01 s). (ρ/ρ_0) is assumed to be unity, and

$$\eta_{sp} = \eta_{rel} - 1 \quad (2)$$

$$\eta_{red} = \eta_{sp}/c \quad (3)$$

A plot η_{red} vs. concentration yields the intrinsic viscosity, $[\eta]$ at the intercept and the slope is related to the concentration dependence, k_H (Huggins, 1942).

$$\eta_{red} = [\eta]\,(1 + k_H[\eta]c) \quad (4)$$

Alternatively, the Kraemer method of plotting $\ln(\eta_{rel})$ vs. concentration can also be used to calculate the intrinsic viscosity and the corresponding Kraemer constant, k_K (see e.g. Harding, 1998).

$$(\ln \eta_{rel})/c = [\eta](1 - k_K[\eta]c) \quad (5)$$

2.3. Rotational viscometry

AH-EPS and xanthan samples of various concentrations (0.1–1.5 and 0.1–1.2 mg/ml, respectively) were prepared in 1 M GuHCl. The viscosity at 25°C was measured using a controlled stress rheometer (CS10, Bohlin) fitted with a double gap geometry (DG40/50). The shear rate used was in the range 0.5–160 s^{-1}.

The set of data was then fitted with the Cross-equation, (Cross, 1965)

$$(\eta_0 - \eta)/(\eta - \eta_\infty) = K\dot{\gamma}^m \quad (6)$$

where η_0 is the zero shear viscosity, η_∞ the high shear viscosity, K and m two constants. The four fitting parameters were optimised to minimise the value of

$$\sum(\log(\eta_f) - \log(\eta))^2 \quad (7)$$

where η_f is the fitted value for each point. The intrinsic viscosity can be obtained via Eqs. (4) and (5).

2.4. Sedimentation velocity (sedimentation-time derivative method)

The Optima XLI (Beckman Instruments, Palo Alto, USA) equipped with Rayleigh interference optics was used to determine the sedimentation behaviour of the saccharide samples. Rotor speeds of 40,000 rpm and a 4 mm column length in 12 mm optical path length double sector cells were used together with an accurately controlled temperature of 25.0°C. A typical polysaccharide weighted average partial specific volume, $\bar{\nu}$ of (0.600 ± 0.005 ml/g) was used for both bacterial polysaccharide samples, this is consistent with previous xanthan studies (Dhami et al., 1995; Sato, Norisuye & Fujita, 1984). The so-called $g^*(s)$ (sedimentation time derivative) method (Stafford, 1992) was used to determine apparent sedimentation coefficients at each concentration. As the sedimenting boundary moves towards the cell base the change in concentration (of the sedimenting species) over time (dc/dt) is calculated from the subtraction

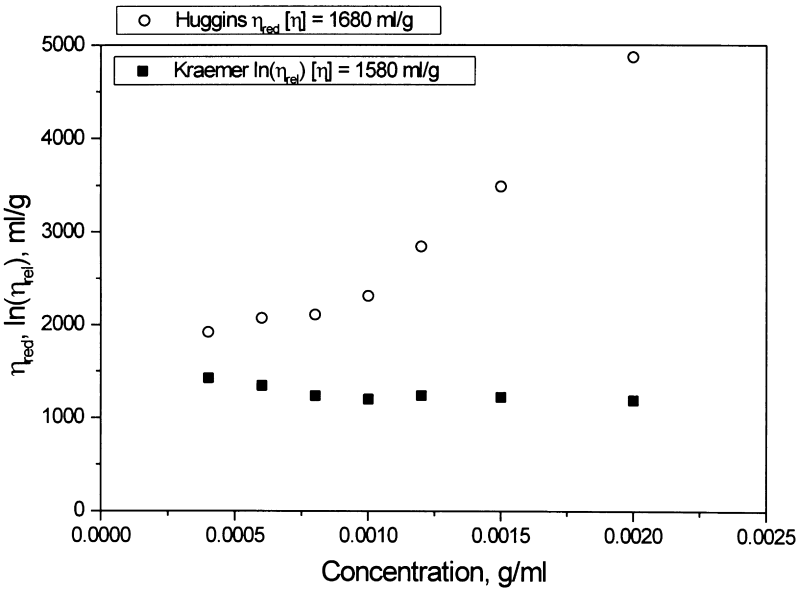

Fig. 1. Huggins and Kraemer plots for AH-EPS from capillary viscometry. Values for [η] will be underestimates (see text).

of multiple pairs of scans (maximum 20 pairs): an apparent distribution $g^*(s)$ of sedimentation coefficients can in this way be produced (Stafford, 1992), where the "*" indicates "apparent" in the sense of not being corrected for diffusion effects nor non-ideality. The apparent *weight average* sedimentation coefficient, s^* can then be calculated (Stafford, 1992), corresponding to particular buffer conditions and temperature (T). From this, normalisation to $s_{20,w}$ values (i.e. to the density and viscosity of water at 20.0°C) can then be performed, according to the standard equation (see e.g. Ralston, 1993):

$$s_{20,w} = s^*[(1 - \bar{v}\rho_{20,w})\eta_{T,b}]/[(1 - \bar{v}\rho_{T,b})\eta_{20,w}] \quad (8)$$

where $\eta_{T,b}$, $\eta_{20,w}$ are, respectively, the viscosities of the solvent at temperature T and water at 20.0°C, and $\rho_{T,b}$ and $\rho_{20,w}$, the corresponding solvent densities.

$s_{20,w}$ values were evaluated at various concentrations from 0.5 to 3.0 mg/ml and extrapolated to zero concentration (to remove the effects of non-ideality) using the standard equations (see e.g. Ralston, 1993).

$$s_{20,w} = s^0_{20,w}(1 - k_s c) \quad (9)$$

$$1/s_{20,w} = (1/s^0_{20,w})(1 + k_s c) \quad (10)$$

where the Gralen parameter (Gralen, 1944), k_s is a measure of concentration dependence.

2.5. Sedimentation equilibrium

The Beckman Optima XLI ultracentrifuge was also used also to determinate the weight average molecular weight, M_w using low speed sedimentation equilibrium. A rotor speed of 3000 rpm and a 1 mm solution column length in 12 mm path length double sector cells were employed at a running temperature of 25.0°C. Equilibrium was reached after approximately 72 h. Rayleigh interference optics were used to record the solute distributions at sedimentation equilibrium and data subsequently analysed using the QUICKBASIC algorithm MSTARI (Cölfen & Harding, 1997).

This program estimates

(i) molecular weight for the whole distribution of solute in the ultracentrifuge cell (from meniscus to cell base) using the operational point average, the "star average" M^*, and the identity M^* (cell base) = $M_{w,app}$. (the apparent weight average molecular weight).
(ii) the apparent point average weight average molecular weight as a function of radial position, $M_{w,app}(r)$. These values are obtained by the sliding strip procedure as described in Teller (1973).

Since interference optical records are of concentration relative to the meniscus, the meniscus concentration needs to be calculated before absolute concentrations can be obtained and (i) and (ii) subsequently performed. For this, the "intercept over slope" method as described in Creeth and Harding (1982) was employed in the initial stage of running MSTARI. In order to account for thermodynamic non-ideality, calculated apparent molecular weights should be extrapolated to zero concentration.

$$1/M_{w,app} = 1/M_w + 2Bc \quad (11)$$

where B is the 2nd thermodynamic (osmotic pressure) virial coefficient.

3. Results and discussion

3.1. Capillary viscometry for AH-EPS

There appears to be a discontinuity in the graph at concentrations above 1 mg/ml: it is likely that this is a result of the effect of shear thinning on polysaccharide solutions, especially at low concentrations (Launay, Cuvelier & Martinez-Reyes, 1997). It is also probable that an increase in viscosity is due to the transition from the dilute to the semi-dilute regimes i.e. a c^*, the critical coil overlap concentration effect (Fig. 1). It was therefore considered best to use the low concentrations for the extrapolations (Dhami et al., 1995). Because of the large viscosities however shear thinning effects are, as with xanthan (Launay et al., 1997) likely leading to a considerable underestimate for [η].

3.2. Capillary viscometry for xanthan

The experiment above was repeated using a well characterised (in water) bacterial polysaccharide—xanthan. Due to the large shear thinning effect in the capillary no meaningful results can be calculated. It could, however, be inferred that the shear-thinning behaviour of AH-EPS in the capillary is similar to that of xanthan. This is consistent with the findings of Cesaro et al. (1990) and Navarini et al. (1990) in their studies of the chemically similar exopolysaccharide CC-EPS.

3.3. Rotational viscometry for AH-EPS

The data obtained at low shear rate and low concentrations were discarded due to the noise level. The viscosities obtained at high shear rate and low concentration were also discarded due to turbulence (Fig. 2a). Although the raw data does not reach a higher Newtonian plateau, the η_0 value obtained by the fitting of the Cross-equation was remarkably reliable. Extrapolation to zero concentration gives an intrinsic viscosity of 8200 and 7900 ml/g, respectively, from the Kraemer and Huggins plots (Fig. 2b). An estimation of the coil overlap concentration, c^* is independent of the intrinsic viscosity and can therefore be measured without creating a bias, a c^* of 0.73 mg/ml was found for AH-EPS (Fig. 2c).

3.4. Rotational viscometry for xanthan

No curvature was observed at low shear rates for the xanthan sample. It was therefore impossible to fit the data via the Cross-equation and calculate an intrinsic viscosity under the experimental conditions.

3.5. Sedimentation velocity (sedimentation-time derivative method)—AH-EPS

The analysis of the sedimenting boundary indicated that the solution was almost entirely homogeneous with only a small amount of aggregated material (Fig. 3a). As with the

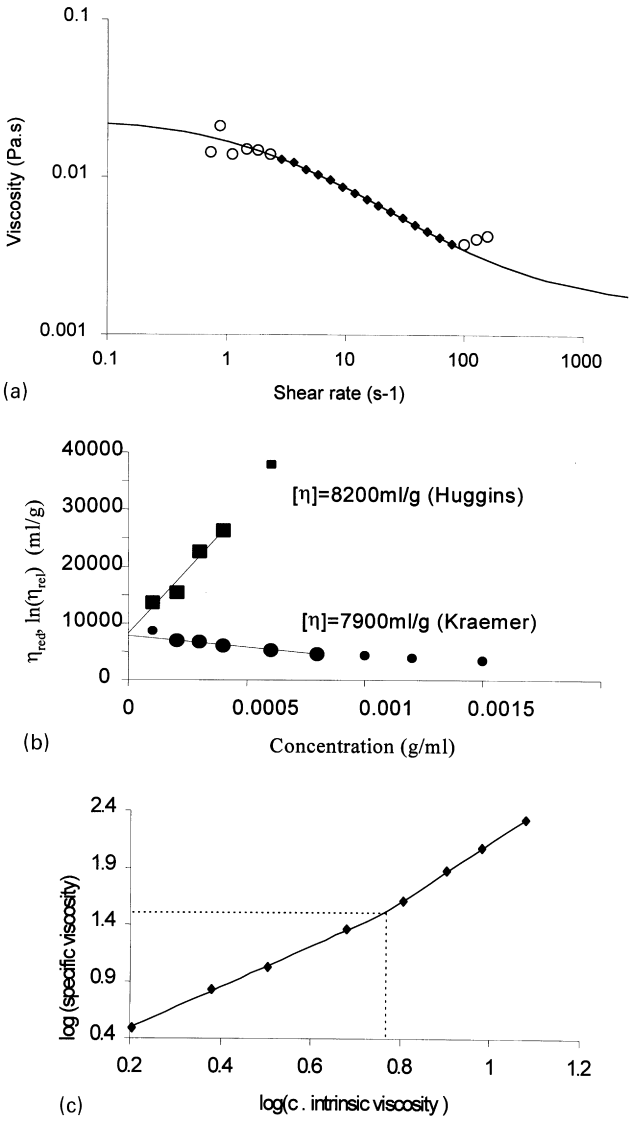

Fig. 2. (a) Viscosity and fitting of AH-EPS at 0.6 g/l measured at 25°C. Circles: points not used for fitting. Square: points used for fitting. Line: fitted curve. (b) Huggins (square) and kraemer (circle) plots for AH-EPS. Extrapolation towards zero concentration was performed on the points with a large marker. (c) Coil overlap plot obtained with an intrinsic viscosity value of 8000 ml/g.

viscometry results a apparent discontinuity can be seen around 1 mg/ml (Fig. 3b and c): this is fairly consistent with the c^* of 0.7 mg/ml calculated from zero-shear viscosity estimates using the Cross-equation. Therefore only the lowest three concentrations were used to estimate the infinite dilution sedimentation coefficient, $s^0_{20,w}$ and the concentration dependency, k_s. Although the sedimentation coefficients are in reasonable agreement and the concentration dependencies are quite different. In general values k_s from the reciprocal plot (Fig. 3c) are more reliable in non-ideal systems (see e.g. Harding, 1995). The results from sedimentation velocity indicate that AH-EPS is a large non-ideal, rigid/extra-rid rod-like polysaccharide. This was also supported by the formation of classical hyper-sharp

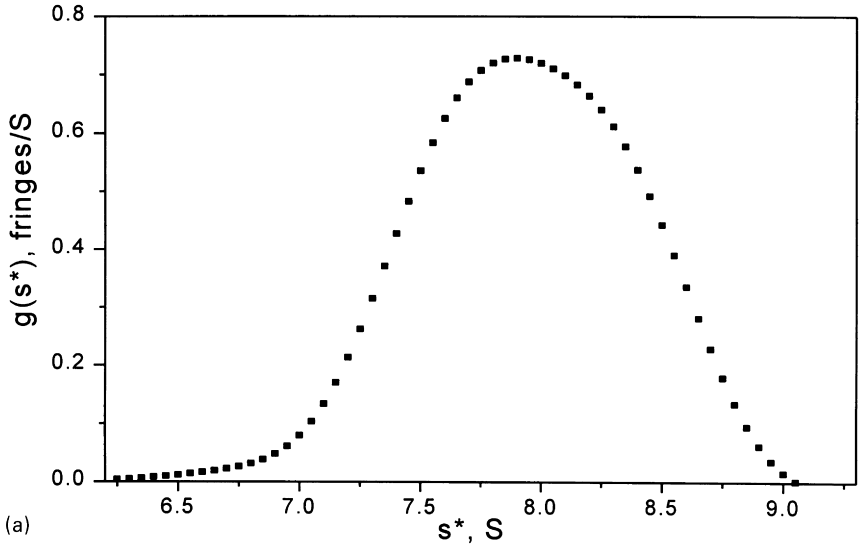

(a)

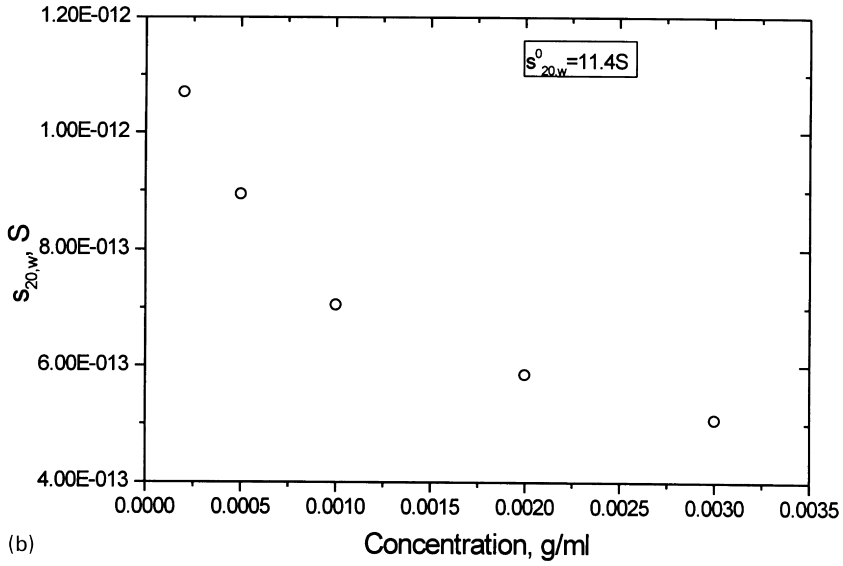

(b)

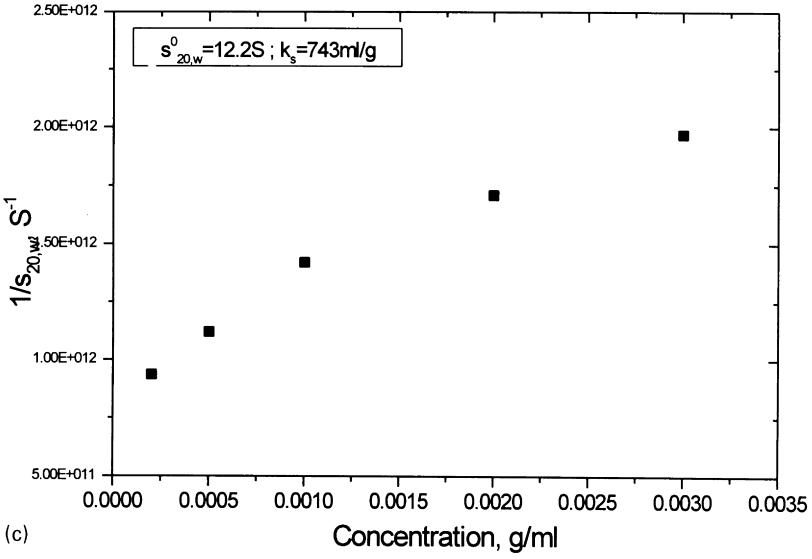

(c)

Fig. 3. (a) $g(s^*)$ profile for AH-EPS—1.0 mg/ml. (b) Concentration dependency of sedimentation-conventional plot. (c) Concentration dependency of sedimentation-reciprocal plot.

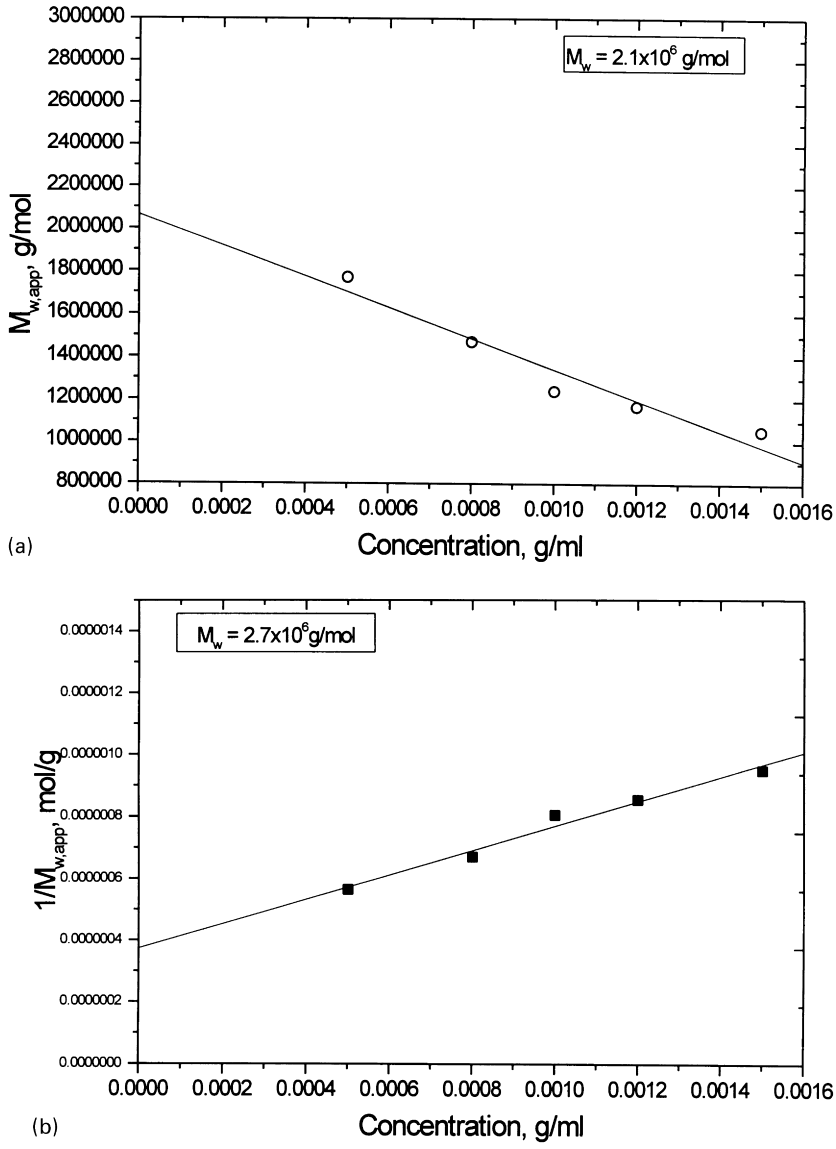

Fig. 4. (a) Concentration dependency of apparent molecular weight-conventional plot. (b) Concentration dependency of apparent molecular weight-reciprocal plot.

boundaries. This is quite different with observations that the solution conformation of the related exopolysaccharide from *Cyanospora capsulata* (CC-EPS) is a random coil (Cesaro et al., 1990; Navarini et al., 1992).

3.6. Sedimentation velocity (sedimentation-time derivative method)—xanthan

Similar shaped hyper-sharp boundaries were observed indicating that AH-EPS and xanthan have similar rigid conformations. A sedimentation coefficient, $s^0_{20,w}$ of 11.4S is quite similar to those observed in pH 6.5 $I = 0.3$ buffer (Dhami et al., 1995) and only slightly smaller than that of AH-EPS. (Table 1)

3.7. Sedimentation equilibrium—AH-EPS

Unlike the viscometry and sedimentation velocity, there appears to be no effect of c^* on sedimentation equilibrium. Molecular weights were therefore extrapolated over the entire concentration range (Fig. 4a and b). Results are again consistent with a non-ideal system.

3.8. Sedimentation equilibrium—xanthan

As with AH-EPS, there is no effect of c^* on sedimentation equilibrium. Molecular weights are again consistent with those of Dhami et al. (1995) $(5.9 \pm 0.6) \times 10^6$ g/mol. However, the 2nd thermodynamic virial coefficient, B is twice as large for AH-EPS, but $2BM$ is larger for xanthan.

Table 1
Experimental and calculated parameters for AH-EPS and xanthan in 1 M guanidine hydrochloride

Hydrodynamic parameter	AH-EPS	Xanthan
$[\eta]$, (from capillary), ml/g	1630 ± 100	–
$[\eta]$, (from Bohlin), ml/g	8000 ± 200	–
c^*, (from Bohlin), g/ml	0.00073 ± 0.00004	–
$s^0_{20,w}$ (from plot of s vs. c), S	11.4 ± 0.4	10.9 ± 0.3
$s^0_{20,w}$ (from plot of $1/s$ vs. c), S	12.2 ± 0.1	11.8 ± 0.8
k_s (from plot of $1/s$ vs. c), ml/g	743 ± 5	540 ± 30
$10^{-6} \times M_w$ (from M_{wapp} vs. c), g/mol	2.1 ± 0.2	4.8 ± 0.2
$10^{-6} \times M_w$ (from $1/M_{wapp}$ vs. c), g/mol	2.7 ± 0.2	6.9 ± 0.6
$10^4 \times B$ (from $1/M_{wapp}$ vs. c), ml.mol/g^2	2.0 ± 0.1	1.0 ± 0.1
2BM (from $1/M_{wapp}$ vs. c), ml/g	1100 ± 150	1400 ± 250
f/f_0, (from plot of s vs. c and $1/M_{wapp}$ vs. c)	9.7 ± 0.8	19.0 ± 2.0
$R = k_s/[\eta]$, (from Bohlin and plot of $1/s$ vs. c)	0.10 ± 0.01	–
$\Pi = 2BM/[\eta]$, (from Bohlin and $1/M_{wapp}$ vs. c)	0.14 ± 0.02	–

4. Conclusions

Our data would suggest that AH-EPS, though chemically different is physically similar in its properties to xanthan. This is particularly true of the results from viscometry (both capillary and double gap) and for sedimentation velocity. Both samples show classic shear thinning behaviour over a large concentration range, as well as the existence of a critical coil overlap concentration, c^*. This together with the formation of hyper-sharp boundaries during sedimentation velocity indicates that both AH-EPS and xanthan are large extra rigid or rigid rod polysaccharides (Pavlov, Rowe & Harding, 1997). The greater molecular weight of xanthan would indicate a greater degree of extension than AH-EPS due to the larger translational frictional ratio, f/f_0 (Tanford, 1961) a parameter which depends on conformation and molecular hydration (Table 1).

$$(f/f_0) = M_w(1 - \bar{v}\rho_0)/(N_A 6\pi\eta_0 s^0_{20,w})(4\pi N_A/3\bar{v}M_w)^{1/3} \quad (12)$$

where N_A is the Avogadro's number and η_0 and ρ_0 the viscosity and density of water at 20.0°C, respectively.

Due to the unreliability of intrinsic viscosity measurements from capillary viscometry it is only possible to estimate the Wales-van Holde ratio, $R = k_s/[\eta]$ or the Π function, $2BM/[\eta]$ from the Bohlin measurements. The small values for each function therefore indicate that AH-EPS is an extended rod-like molecule (Dhami et al., 1995; Harding & Cölfen, 1995; Harding, Berth, Ball, Mitchell & Garcia de la Torre, 1991) of the zone A type (Pavlov et al., 1997) of axial ratio, a/b greater than 100.

The data suggests that like many exobacterial polysaccharides AH-EPS does exhibit xanthan-like properties (at least in the solvent system studied) and could be industrially useful, this is, however, dependent on the cost effectiveness of extraction and purification. It is clear that the poor solubility of AH-EPS in many traditional solvents puts great limitations on any industrial applications. It should also be noted that there are many stages in the purification process (drying etc.) where AH-EPS may have undergone modification of some form.

References

Bar, E., & Visnovsky, S. (1997). Development of an algal biomatrix as a natural solution for improving soil characteristics and for land stabilization. *Phycologia, (Suppl.)*, *36*, 5.

Bar-or, Y., & Shilo, M. (1987). Characterization of marcromolecular flocculants produced by Phormidium sp. StrainJ-1 and by *Anabaenopsis circularis* PCC6720. *Applied Environmental Microbiology*, *53*, 2226–2230.

Brock, T. D. (1976). Halophilic blue-green algae. *Archives in Microbiology*, *107*, 109–111.

Cesaro, A., Liut, G., Bertocchi, C., Navarini, L., & Urbani, R. (1990). Physicochemical properties of the exocellular polysaccharide from *Cyanospira capsulata*. *International Journal of Biology and Macromol.*, *12*, 79–84.

Choi, W. C., Yoo, S., Oh, I., & Park, S. H. (1998). Characterization of an extracellular flocculating substance produced by a planktonic cyanobacterium, *Anabaena* sp. *Biotechnology Letters*, *20*, 643–646.

Cölfen, H., & Harding, S. E. (1997). MSTARA and MSTARI: interactive PC algorithms for simple, model independent evaluation of sedimentation equilibrium data. *European Biophysics Journal*, *25*, 333–346.

Creeth, J. M., & Harding, S. E. (1982). Some observations on a new type of point average molecular weight. *Biochemical and Biophysical Methods*, *7*, 25–34.

Cross, M. M. (1965). Rheology of non-Newtonian fluids: a new flow equation for pseudoplastic systems. *Journal of Colloid Sciences*, *20*, 417–437.

De Philippis, R., & Vincenzini, M. (1998). Exocellular polysaccharides from cyanobacteria and their possible applications. *FEMS Microbiology Reviews*, *22*, 151–175.

Dhami, R., Harding, S. E., Jones, T., Hughes, T., Mitchell, J. R., & To, K. (1995). Physico-chemical studies on a commercial food grade xanthan-I. Characterisation by sedimentation velocity, sedimentation equilibrium and viscometry. *Carbohydrate Polymers*, *27*, 93–99.

Drews, G., & Weckesser, J. (1982). Function, structure and composition of cell walls and external layers. In N. G. Carr & B. A. Whitton, *The biology of cyanobacteria* (pp. 333–357). , Vol 19. Oxford: Blackwell.

Falchini, L., Sparvoli, E., & Tomaselli, L. (1996). Effect of *Nostoc* (Cyanobacteria) inoculation on the structure and stability of clay soils. *Biology of Fertile Soils*, *23*, 346–352.

Garozzo, D., Impallomeni, G., Spina, E., & Sturiale, L. (1998). The structure of the exopolysaccharide from the cyanobacterium *Cyanospira capsulata*. *Carbohydrate Research*, *307*, 113–124.

Gralen, N., PhD dissertation, University of Uppsala, Sweden, 1944.

Green, A. A. (1933). The preparation of acetate and phosphate buffer

solutions of known pH and ionic strength. *Journal of the American Chemical Society*, *55*, 2331.

Harding, S. E. (1995). Some recent developments in the size and shape analysis of industrial polysaccharides in solution using sedimentation analysis in the analytical ultracentrifuge. *Carbohydrate Polymers*, *28*, 227–237.

Harding, S. E. (1998). The intrinsic viscosity of biological macromolecules. progress in measurement, interpretation and application to structure in dilute solutions. *Progress in Biophysics and Molecular Biology*, Vol. 68. Amsterdam: Elsevier (pp. 207–262).

Harding, S. E., & Cölfen, H. (1995). Inversion formulae for ellipsoid of revolution macromolecular shape functions. *Analytical Biochemistry*, *228*, 131–142.

Harding, S. E., Berth, G., Ball, A., Mitchell, J. R., & Garcia de la Torre, J. (1991). The molecular-weight distribution and conformation of citrus pectins in solutions studied by hydrodynamics. *Carbohydrate Polymers*, *16*, 1–15.

Huggins, M. L. (1942). The viscosity of long chain molecules IV: dependence on concentration. *Journal of the American Chemical Society*, *64*, 2716–2718.

Launay, B., Cuvelier, G., & Martinez-Reyes, S. (1997). Viscosity of locust bean, guar and xanthan gum solutions in the Newtonian domain: a critical examination of the $\log(\eta_{sp})_0$–$\log C[\eta]_0$ master curves. *Carbohydrate Polymers*, *34*, 385–395.

Li, P., Liu, Z., Xu, R., Zhu, H. (2000). Submitted for publication.

Liu, Z., & Lin, H. (1993). A species of microalgal with useful and developable prospects—*Aphanothece halophytica*. *Sea-lake Salt & Chemical Industry*, *22*, 16–19.

Marra, M., Palmeri, A., Ballio, A., Segre, A., & Slodki, M. E. (1990). Structural characterisation of the exopolysaccharide from *Cyanospira capsulata*. *Carbohydrate Research*, *197*, 338–344.

Mazor, G., Kidron, G. J., Vonshak, A., & Abeliovich, A. (1996). The role of cyanobacterial exopolysaccharides in structuring desert microbial crusts. *FEMS Microbiology and Ecology*, *21*, 121–130.

Navarini, L., Bertocchi, C., Cesaro, A., Lapasin, R., & Crescenzi, V. (1990). Rheology of aqueous solutions of an extracellular polysaccharide from *Cyanospira capsulata*. *Carbohydrate Polymers*, *122*, 169–187.

Navarini, L., Cesaro, L., & Ross-Murphy, S. B. (1992). Viscoelastic properties of aqueous solutions of an exocellular polysaccharide from cyanobacteria. *Carbohydrate Polymers*, *18*, 265–272.

Nicolaus, B., Panico, A., Lama, L., Romano, I., Manca, M. C., De Giulio, A., & Gambacorta, A. (1999). Chemical composition and production of exopolysaccharides from representative members of heterocystous and non-heterocystous cyanobacteria. *Phytochemistry*, *52*, 639–647.

Pavlov, G. M., Rowe, A. J., & Harding, S. E. (1997). Conformation zoning of large molecules using the analytical ultracentrifuge. *Trends in Analytical Chemistry*, *16* (7), 401–405.

Ralston, G. (1993). Introduction to analytical ultracentrifugation. Beckman Instruments Inc., CA.

Sato, T., Norisuye, T., & Fujita, H. (1984). Double-stranded helix of xanthan in dilute-solution—further evidence. *Polymer Journal*, *16*, 423–429.

Stafford, W. F. (1992). Methods for obtaining sedimentation coefficient distributions. In S. E. Harding, A. J. Rowe & J. C. Horton, *Analytical ultracentrifugation in biochemistry and polymer science*Cambridge: Royal Society of Chemistry (chap. 20).

Tanford, C. (1961). *Physical chemistry of macromolecules*, New York: Wiley (chap. 6).

Teller, D. C. (1973). Characterisation of proteins by sedimentation equilibrium in the analytical ultracentifuge. *Methods in Enzymology*, *27*, 346–441.